

Efficient electromagnetic analysis of two-dimensional finite quasi-random gratings for quantum well infrared photodetectors

Vikram Jandhyala,^{a)} Deepak Sengupta, Balasubramaniam Shanker, Eric Michielssen, Milton Feng, and Greg Stillman

Department of Electrical and Computer Engineering, 1406 West Green Street, University of Illinois at Urbana-Champaign, Urbana, Illinois 61801

(Received 18 August 1997; accepted for publication 9 December 1997)

In this work, a recently developed full-wave electromagnetic analysis technique is applied to the simulation of two-dimensional finite quasi-random gratings for quantum well infrared photodetectors. This steepest descent fast multipole method is a mathematically rigorous technique that permits the rapid and accurate solution of the electric field integral equation governing scattering from a quasi-planar structure. In the present application, it enables the efficient and accurate simulation of scattering by finite two-dimensional grating structures interfacing with GaAs. Grating absorption is predicted by evaluating the scattered optical electric field component at the device layer along the growth direction. Numerical examples illustrating the functional dependence of the absorption on grating parameters and wavelength are discussed. The simulation approach presented here should prove to be a useful tool for the *a priori* design of novel aperiodic, quasi-random and rough surface two-dimensional gratings for infrared imaging applications.
© 1998 American Institute of Physics. [S0021-8979(98)07806-2]

INTRODUCTION

Quantum well infrared photodetectors (QWIPs) with AlGaAs/GaAs quantum wells have shown great potential as sensors in large imaging arrays.¹⁻⁵ Owing to quantum mechanical selection rules, most unstrained *n*-type QWIPs respond only to the longitudinal component of the optical electrical field, i.e., the field along the growth direction. For such devices to sense normally incident radiation, optical grating couplers are necessary to scatter the optical field in directions favorable to intersubband absorption.⁶⁻¹¹ While periodic gratings⁶⁻⁹ have been extensively studied and modeled using modal expansion methods, aperiodic or quasi-random gratings^{10,11} have not been analyzed in comparable detail. Nonetheless, quasi-random gratings have been experimentally observed to produce better absorption over broad spectral ranges than periodic ones. The necessarily large but finite dimensions of realistic gratings place an exacting demand on solution efficiency and accuracy, since the computational advantages of small-scale problems or the relative ease of infinite approximations disappear. Unfortunately, the computational burden associated with the solution of a large-scale, three-dimensional, vector electromagnetic problem has restricted the numerical analysis of quasi-random gratings to modal expansions for computationally simpler one-dimensional profiles.¹¹

In this paper, a recently developed accurate and efficient integral equation based technique is applied to the analysis of finite two-dimensional quasi-random gratings. This technique, termed the steepest descent fast multipole method (SDFMM),¹² is based on an alternate representation of the dyadic Green's function governing free space electromagnetic radiation using a steepest descent integral form and

inhomogeneous plane wave expansions. Such an approach permits a fast and memory efficient iterative solution of the integral equation associated with scattering from quasi-planar structures.

FORMULATION

The back-illuminated QWIP structure to be analyzed is shown in Fig. 1(a). The metallic grating layer *S* (modeled as a perfect conductor^{8,11}), which interfaces with GaAs, prevents radiation loss and serves as a contact. An optical wave impinges normally on the grating from the substrate side, and the scattered wave excites the quantum wells owing to its non-zero electric field along the growth direction. The incident field $\mathbf{E}_{\text{inc}}(\mathbf{r})$ is assumed to be a tapered Gaussian beam,¹³ which suppresses edge scattering effects at the mesa boundary. This assumption is consistent with the observation that a substantial portion of the grating and device near the mesa edge is optically inactive.⁸ A surface current $\mathbf{J}(\mathbf{r})$ is generated at the grating due to $\mathbf{E}_{\text{inc}}(\mathbf{r})$. The total electric field tangential to *S* must vanish on *S*, and hence the following integral equation holds:

$$\hat{\mathbf{t}}(\mathbf{r}) \cdot \mathbf{E}_{\text{scat}}(\mathbf{r}, \mathbf{J}) = -\hat{\mathbf{t}}(\mathbf{r}) \cdot \mathbf{E}_{\text{inc}}(\mathbf{r}) \quad \mathbf{r}, \mathbf{r}' \in S, \quad (1a)$$

with

$$\mathbf{E}_{\text{scat}}(\mathbf{r}, \mathbf{J}) = \frac{k_0 \eta_0}{i} \int_S \bar{\mathbf{G}}(\mathbf{r}, \mathbf{r}') \cdot \mathbf{J}(\mathbf{r}') dS' \quad \mathbf{r} \in S, \quad (1b)$$

where k_0 and η_0 are the free-space wave number and impedance, $\hat{\mathbf{t}}(\mathbf{r})$ denotes a unit tangent to *S* at \mathbf{r} , and $\bar{\mathbf{G}}(\mathbf{r}, \mathbf{r}')$ is the free-space dyadic Green's function.¹⁴

The solution of Eq. (1) yields $\mathbf{J}(\mathbf{r})$, and the total longitudinal electric field at the device layer can then be obtained via $\bar{\mathbf{G}}(\mathbf{r}, \mathbf{r}')$. A standard approach to solving Eq. (1) is to use the method of moments (MoMs),¹⁵ wherein $\mathbf{J}(\mathbf{r})$ is expressed as a linear combination of basis functions $\mathbf{j}_n(\mathbf{r})$, $n = 1, \dots, N$ as

^{a)}Electronic mail: vikram@decwa.ece.uiuc.edu

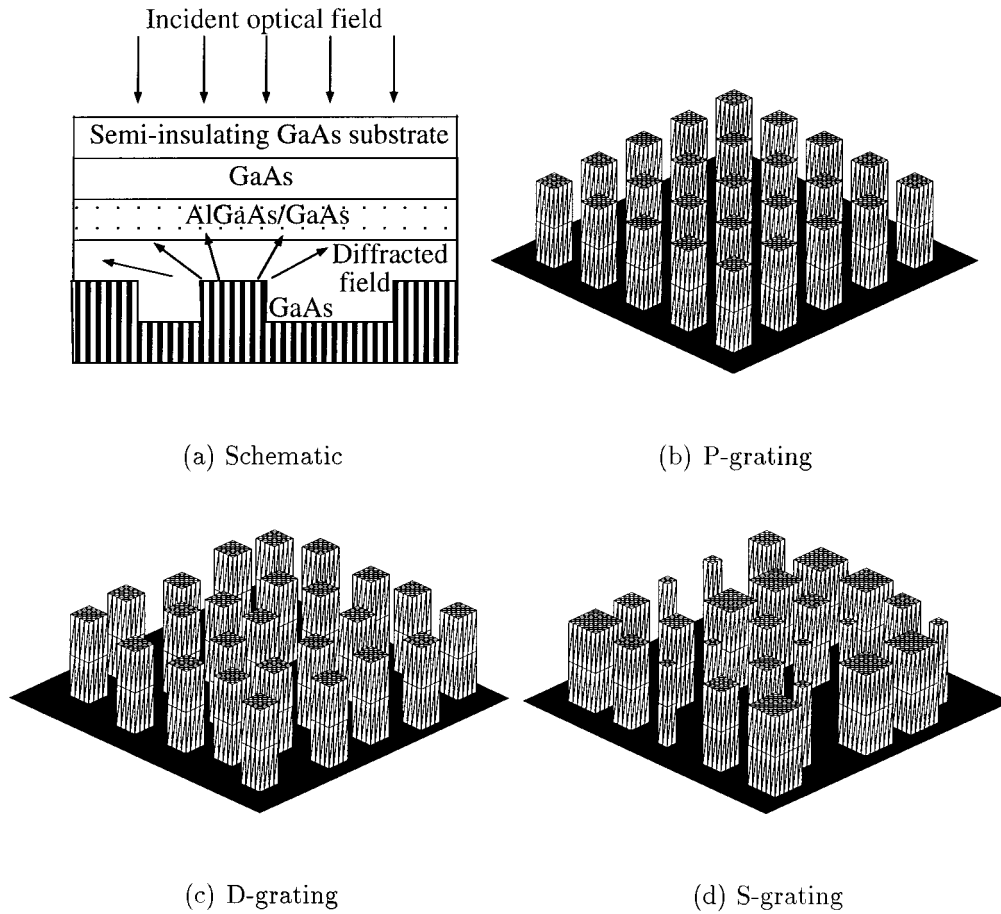


FIG. 1. (a) Schematic cross section view of the grating coupled QWIP device. (b) Periodic (P) grating. (c) Displaced (D) grating. (d) Scaled (S) grating. One corner of each raised portion is fixed, while the other corner is shifted diagonally.

$$\mathbf{J}(\mathbf{r}) \cong \sum_{n=1}^N I_n \mathbf{j}_n(\mathbf{r}). \quad (2a)$$

Subsequently testing the resulting equations with a set of functions $\mathbf{f}_m(\mathbf{r})$, $m = 1, \dots, N$ leads to a dense matrix equation of order N of the form

$$\bar{\mathbf{Z}} \cdot \mathbf{I} = \mathbf{V}, \quad (2b)$$

with

$$Z_{mn} = \langle \mathbf{f}_m(\mathbf{r}), \mathbf{E}_{\text{scat}}(\mathbf{r}, \mathbf{j}_n) \rangle, \quad (2c)$$

and

$$V_m = \langle \mathbf{f}_m(\mathbf{r}), \mathbf{E}_{\text{inc}}(\mathbf{r}) \rangle, \quad (2d)$$

where $\langle \cdot, \cdot \rangle$ denotes surface integration. A popular choice for the functions $\mathbf{j}_n(\mathbf{r})$ and $\mathbf{f}_m(\mathbf{r})$ is the Rao-Wilton-Glisson (RWG) basis,¹⁶ which will be utilized here. For a grating of size $L \times L$ square wavelengths, N grows approximately as $200L^2$. For the QWIP grating structure under analysis, N can be of the order of 10^4 or 10^5 . Hence, direct inversion of $\bar{\mathbf{Z}}$, which entails a computational cost proportional to N^3 , is practically impossible. An iterative solution has a cost proportional to N^2 per iteration, which also prohibits the solution of large problems. Moreover, both these approaches require the storage of $\bar{\mathbf{Z}}$, necessitating memory requirements

proportional to N^2 . The SDFMM, a hybrid between the fast steepest descent path algorithm¹⁷ and the two-dimensional multilevel fast multipole method,¹⁸ relies on a hierarchical decomposition of the scatterer into blocks at several levels of coarseness. In the SDFMM, the elements of the MoM matrix $\bar{\mathbf{Z}}$ are formally expressed as

$$\begin{aligned} Z_{mn}'' \cong & \sum_{j=1}^{n_{sd}} \sum_{j'=1}^P w_j^{sd} w_{j'}^{fmm} \int_S d\mathbf{r} \mathbf{f}_m(\mathbf{r}) e^{i\mathbf{k}^{(j)} \cdot (\mathbf{r} - \mathbf{r}_t)} \\ & \times \mathcal{T}_{jj'}(\mathbf{r}_t - \mathbf{r}_s) \left(\bar{\mathbf{I}} - \frac{\mathbf{k}^{(j)} \mathbf{k}^{(j)}}{k_0^2} \right) \int_S d\mathbf{r}' \mathbf{j}_n(\mathbf{r}') \\ & \times e^{i\mathbf{k}^{(j)} \cdot (\mathbf{r}_s - \mathbf{r}')}, \end{aligned} \quad (3)$$

where $\mathbf{k}^{(j)}$ are complex wave numbers, and n_{sd} and w_j^{sd} are the number of points and integration weights associated with integration along the steepest descent path of the Sommerfeld integral representation of the free-space Green's function.¹² Source and testing block centers are denoted by \mathbf{r}_s and \mathbf{r}_t , respectively. The translation operator $\mathcal{T}_{jj'}(\mathbf{r}_t - \mathbf{r}_s)$, integration weights $w_{j'}^{fmm}$, and number of harmonics P are analogous to those defined in well known fast multipole algorithms.¹⁸⁻²¹ The SDFMM enables the aggregation and disaggregation of basis and testing functions through the

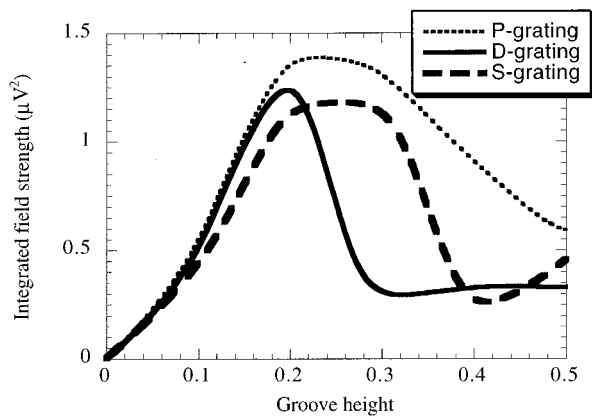


FIG. 2. Integrated field strength vs groove height for P , D , and S gratings. The groove height is in wavelengths.

two far-field integrals appearing in Eq. (3). This results in a dramatic reduction in the complexity of matrix-vector products involving $\bar{\mathbf{Z}}$ and memory requirements from $O(N^2)$ to $O(N)$.

NUMERICAL RESULTS

Three kinds of periodic and quasi-random gratings, shown in Fig. 1, have been studied. The P -grating [Fig. 1(b)] is a doubly *periodic* grating. *Displacing* raised portions of this grating produces a D grating [Fig. 1(c)], while *scaling* raised portions of a P -grating generates an S grating [Fig. 1(d)]. The P , D , and S gratings used here are $38 \times 38 \mu\text{m}$. As a precursor to employing the RWG basis in conjunction with the SDFMM, the grating surfaces are tessellated into planar triangles, with the nodes separated by approximately 0.14λ , where λ is the optical wavelength in the GaAs layer. For infrared radiation with a free-space wavelength of $10 \mu\text{m}$, $\lambda \cong 3.03 \mu\text{m}$. Current on each grating is modeled in terms of approximately $N = 30\,000$ basis functions. With the SDFMM, such a problem can be solved in 3–7 hours (depending on the number of iterations required) on a single processor R8000 SGI Power Challenge. Detailed memory and CPU time comparisons for the SDFMM, for standard iterative solvers, and for LU decomposition have been carried out earlier for rough surface scattering problems, and are reported in Ref. 12.

The periodicity of the P grating is $4.0 \mu\text{m}$ along each lateral direction and the raised portions measure $2.0 \times 2.0 \mu\text{m}^2$. The average shift relative to the period size for the specific D grating considered is 14%, and the maximum is 50%. The average deviation in size (relative compression/elongation) for the S grating is 32% and the maximum deviation is 50%. Figure 2 shows the integrated field strength as a function of grating height for the three gratings. A nominal grating period of one wavelength is used for all gratings. The integrated field strength is computed by integrating the square of the longitudinal electric field over the cross section of the QWIP at the device layer. Grating absorption is proportional to this measure.¹¹ As can be seen, the absorption of the P and S gratings is maximum when the grating height is approximately 0.25λ , while the D -grating response peaks at a grating height close to 0.2λ . As in the one-dimensional

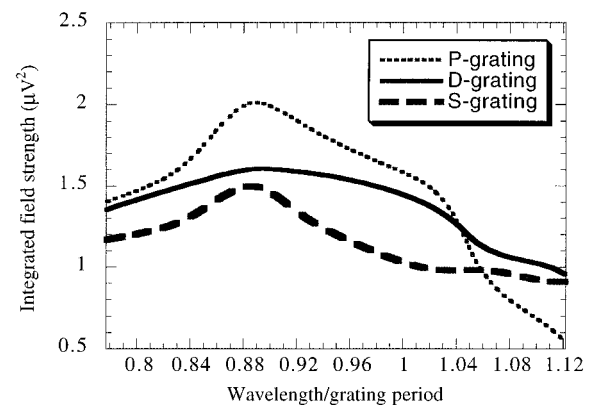


FIG. 3. Integrated field strength vs wavelength/period. The ratios of the maximum to minimum integrated field strength are 3.83, 1.75, and 1.70 for the P , D , and S gratings respectively.

case, the peak absorption due to a P grating is larger than that due to the quasi-random gratings. The importance and need for quasi-random gratings is evident when one observes the spectral behavior of the absorption due to the gratings, which is depicted in Fig. 3. For the P grating, the absorption diminishes rapidly at larger wavelengths, due to the evanescent nature of the higher order Floquet modes. If such a grating were designed to operate optimally at the nominal wavelength of $10 \mu\text{m}$, its performance at the extremal wavelengths ($8 \mu\text{m}$ and $12 \mu\text{m}$) would be poor. The D and S gratings, on the other hand, do exhibit a much smoother spectral behavior over the range of interest, albeit with a slightly reduced peak absorption. Hence there exists a tradeoff between peak absorption and smooth spectral behavior.

CONCLUSIONS

In conclusion, this work reports, to the best of our knowledge, the first application of a rigorous full-wave technique to the performance analysis of two-dimensional quasi-random gratings for QWIPs. The SDFMM, developed earlier for analyzing arbitrary quasi-planar structures, is well suited for analyzing scattering from large-scale gratings because its memory requirements and CPU time per matrix-vector product scale as $O(N)$. Using the SDFMM, it has been shown that there is a tradeoff between peak absorption and spectral smoothness. Introducing randomness into a grating leads to a reduced peak absorption but improves spectral properties, which are important when the wavelengths of interest cover a broad band, such as the popular $8 \mu\text{m}$ – $12 \mu\text{m}$ range. The results presented here are qualitatively consistent with the findings reported by Xing and Liu in Ref. 11, for one-dimensional gratings. Hence, we confirm these authors' conjecture that the aforementioned tradeoff demonstrated for one-dimensional gratings in their work should extend to two-dimensional gratings.

In order to fully exploit the degrees of freedom of two-dimensional gratings, additional randomness can be introduced by scaling/displacing raised portions differently in the two lateral directions. Furthermore, other aperiodic structures derived from a criss-cross, rough surface and multilevel

random height gratings can also be analyzed with the SD-FMM. Cavity and waveguide effects,¹ although not dealt with in this paper, can be analyzed with a multi-region integral equation formulation replacing the two-region formulation presented here. It is expected that the techniques suggested in this paper will assist in the *a priori* design of novel and efficient QWIP gratings.

¹B. Levine, J. Appl. Phys. **74**, R1 (1993).

²C. Bethea *et al.*, IEEE Trans. Electron Devices **40**, 1957 (1993).

³L. Kozlowski *et al.*, IEEE Trans. Electron Devices **38**, 1124 (1991).

⁴S. Gunapala *et al.*, IEEE Trans. Electron Devices **44**, 45 (1997).

⁵W. Beck *et al.*, *Proceedings of the International Society of Optical Engineers* (Miami Beach, FL, 1994).

⁶J. Andersson and L. Lundquist, Appl. Phys. Lett. **59**, 857 (1991).

⁷J. Andersson, L. Lundquist, and Z. Paska, Appl. Phys. Lett. **58**, 2264 (1991).

⁸J. Andersson and L. Lundquist, J. Appl. Phys. **71**, 3600 (1992).

⁹L. Lundqvist *et al.*, Appl. Phys. Lett. **63**, 3361 (1993).

¹⁰G. Sarusi *et al.*, J. Appl. Phys. **76**, 4989 (1994).

¹¹B. Xing and H. Liu, J. Appl. Phys. **80**, 1214 (1996).

¹²V. Jandhyala, E. Michielssen, B. Shanker, and W. Chew, Technical Report No. CCEM-3-97, Center for Computational Electromagnetics, University of Illinois, Urbana (1997).

¹³P. Tran and A. A. Maradudin, Opt. Commun. **110**, 269 (1994).

¹⁴W. C. Chew, *Waves and Fields in Inhomogeneous Media* (IEEE, Piscataway, NJ, 1995).

¹⁵R. Harrington, *Field Computation by Moment Methods* (Krieger, Malabar, FL, 1982).

¹⁶S. M. Rao, D. R. Wilton, and A. Glisson, IEEE Trans. Antennas Propag. **30**, 409 (1982).

¹⁷E. Michielssen and W. Chew, Radio Sci. **31**, 1215 (1996).

¹⁸C. C. Lu and W. C. Chew, Microw. Opt. Technol. Lett. **7**, 466 (1994).

¹⁹N. Engheta, W. D. Murphy, V. Rokhlin, and M. S. Vassiliou, IEEE Trans. Antennas Propag. **40**, 634 (1992).

²⁰R. Coifman, V. Rokhlin, and S. Wandzura, IEEE Antennas Propag. Mag. **35**, 7 (1993).

²¹J. M. Song and W. C. Chew, Microw. Opt. Technol. Lett. **10**, 14 (1995).